Applied Mathematics & Information Sciences
An International Journal

http://dx.doi.org/10.18576/amis/190307

Investigation of Caputo Fractional Modeling for Temporal Variations on Hearing Loss due to Mumps Virus

Siham Ayasrah[1], *Asad Freihat*[2], *Mohammed Alabedalhadi*[2,*], *Mohammed Al-Smadi*[2,3,4], *Shrideh Al-Omari*[5] *and Dumitru Baleanu*[6]

[1] Department of Applied Speech Language Pathology and Audiology, Zarqa University, Zarqa, Jordan
[2] Department of Applied Science, Ajloun College, Al-Balqa Applied University, Ajloun 26816, Jordan
[3] College of Commerce and Business, Lusail University, Lusail, Qatar
[4] Nonlinear Dynamics Research Center (NDRC), Ajman University, Ajman 20550, UAE
[5] Department of Mathematics, Faculty of Science, Al-Balqa Applied University, Salt 19117, Jordan
[6] Department of Computer Science and Mathematics, Lebanese American University, Beirut, Lebanon

Received: 2 Jan. 2024, Revised: 14 Mar. 2024, Accepted: 18 May 2024
Published online: 1 May 2025

Abstract: In this work, we employ Caputo's concept of the fractional derivative to investigate a valid fractional mathematical model to study temporal variations in hearing loss associated with the mumps virus. We present a comprehensive investigation into the existence and uniqueness of solutions using fixed-point theory. The Laplace residual power series approach is proposed to produce numerical solutions, which are compared with existing results to validate efficiency. The study provides insights into the complex relationship between hearing loss and fractional calculus, contributing to epidemiological modeling.

Keywords: Fractional model, Hearing loss, Mumps virus, Laplace residual power series method

1 Introduction

One of the generality common tangible impairments affecting millions of people around the world is hearing loss. Many things can contribute to the development of this disease, including genetics, infections, aging, and exposure to loud noise. Mumps virus, a diffuse viral infection that generally affects the salivary glands, is one such disease that raises hearing loss [1]. The parotid glands, lying near the ears, can turn inflamed when the mumps virus comes into the body. The auditory nerves and inner ear are two neighboring constructions that can turn inflamed due to this infection [2]. Consequently, based on the status of infection and injury to the auditory system, those who evolve mumps may endure temporary or permanent hearing loss [3]. The operations that are the reason for mumps-induced hearing loss are complex and distinct. Critical hair cells in the cochlea, which reveal sound vibrations and transmit auditory signals to the brain, can be directly harmed by the virus [4]. The hearing task is further compromised by likely involvement in the transit of signals from the cochlea to the brain due to edema and soreness of the auditory pathways [5]. Hearing loss that is caused by the mumps can have an extensive field of effects, from tenuous hardness hearing high-frequency sounds to whole deafness. Occasionally, hearing loss is tentative and goes away when the infection dissipates and the inflammatory reaction in the body reduces. To upgrade the quality of life and communication, hearing aids or other assistive tools may be required in appointed cases, such as those with persistent hearing loss. A multidisciplinary plan including rehabilitation treatments, ongoing support, and medical intervention is wanted to spin mumps-induced hearing loss [6]. For mumps patients to have superior likely results and decrease their opportunities of extending hearing problems, early exploration and treatment of the virus is major. Moreover, immunization operations and other public health leads are primary to stem the propagation of mumps and lessen the duplication of hearing loss related to the disease [7].

Realization and handling of hearing loss demand a strong mathematical basis, particularly when it relates to modeling and analysis [8]. By supplying quantitative

* Corresponding author e-mail: mohmdnh@bau.edu.jo

settings to demonstrate the basic mechanisms of hearing loss, mathematical models assist researchers in simulating and predicting the effects of a vast field of variables on auditory tasks, including environmental exposures, virus infection, and genetic predisposition [9]. Researchers are able to illustrate the complex relevancies between biological operations and environmental motives that give rise to hearing loss using mathematical tools including differential equations, statistical analysis, and computational simulations [10]. Moreover, producing customized rehabilitation schedules, therapeutic approaches, and diagnostic devices to meet the certain needs of each patient with hearing loss is made simple meanwhile mathematical modeling. Through the employ of mathematics, researchers and clinicians can gain a deeper understanding of hearing loss, upgrade patient results, improve the quality of life for those affected by hearing loss, and move the field of audiology to more successful interventions [11]. The authors of [12] presented a novel mathematical model that considers a few potential causes of hearing loss and is formulated using the following ordinary differential equations (ODEs):

$$\frac{d\psi_S}{dt} = \mu - \alpha_1\psi_S(t)\psi_L(t) - \alpha_2\psi_S(t) + \alpha_3\psi_R(t), \quad (1)$$

$$\frac{d\psi_L}{dt} = \alpha_1\psi_S(t)\psi_L(t) - \alpha_2\psi_L(t) - \alpha_4\psi_L(t), \quad (2)$$

$$\frac{d\psi_R}{dt} = \alpha_4\psi_L(t) - \alpha_3\psi_R(t) - \alpha_2\psi_R(t), \quad (3)$$

subject to the initial conditions:

$$\psi_S(0) = \psi_S0 \geq 0, \quad \psi_L(0) = \psi_L0 \geq 0, \quad \psi_R(0) = \psi_R0 \geq 0. \quad (4)$$

The proposed model splits the population into three epidemiological classes: $\psi_S(t)$ symbolizes the population class involves the number of susceptible individuals who have exposure to hearing loss due to mumps or any other viral infection, genetic disorders, or due to noise (may be due to social, neural, or environmental causes); $\psi_L(t)$ symbolizes the population class involves the number of infected individuals (infected to hearing loss due to mumps, noise exposure, or due to genetic disorders); and $\psi_R(t)$ symbolizes the population class involves the number of infected individuals who have recovered from hearing loss (which may have happened due to mumps, noise exposure, or due to genetic disorders). The parameters in the model (1)-(3) are defined in Table 1.

The authors in [12] talked about the two causes of hearing loss: social exposure to loudness and infectious Mumps disease. Furthermore, they have demonstrated the problem's existence, positivity, and boundedness. In [13], the authors presented a model of mumps-induced hearing loss in children using the Caputo–Fabrizio fractional-order derivative. They studied the equilibrium points and the reproductions number for the model and proved the existence of a unique solution for the model. Moreover, the authors constructed an approximate solution for the fractional-order model using fractional Euler method. A mathematical model on hearing loss owing to mumps virus infection has been investigated in [14]. The reproduction number of the model was calculated. Furthermore, they studied the effect of noise on the proposed system by using Fourier transform technique. In [15], a fractional model for hearing loss with three fractional operators called Atangana–Baleanu–Caputo, Caputo, and Caputo–Fabrizio derivatives has been presented. They established numerical solutions for the proposed model. In our work, we introduce the following fractional model of mumps-induced hearing loss:

Table 1 Description of the parameters in the model (1)-(3).

Parameter	Description	Value
μ	Population recruitment rate	0.8
α_1	Rate of mumps virus transmission	0.0532
α_2	Population death rate due to natural causes	0.3
α_3	Rate of immunity loss	0.02
α_4	Population recovery rate	0.241

$$\frac{1}{\delta^{(1-\beta)}} D_t^{\beta}\psi_S = \mu - \alpha_1\psi_S(t)\psi_L(t) - \alpha_2\psi_S(t) + \alpha_3\psi_R(t), \quad (5)$$

$$\frac{1}{\delta^{(1-\beta)}} D_t^{\beta}\psi_L = \alpha_1\psi_S(t)\psi_L(t) - \alpha_2\psi_L(t) - \alpha_4\psi_L(t), \quad (6)$$

$$\frac{1}{\delta^{(1-\beta)}} D_t^{\beta}\psi_R = \alpha_4\psi_L(t) - \alpha_3\psi_R(t) - \alpha_2\psi_R(t), \quad (7)$$

subject to the initial conditions:

$$\psi_S(0) = \psi_S0 \geq 0, \quad \psi_L(0) = \psi_L0 \geq 0, \quad \psi_R(0) = \psi_R0 \geq 0. \quad (8)$$

The parameter δ is an auxiliary parameter utilized to make the sides of the equations in the model (5)-(7) have the same dimension [16]. In our model (5)-(7), the symbol D_t^{β} denotes the Caputo fractional derivative with respect to time t of order $0 < \beta < 1$. Our work investigates a novel use of Caputo fractional modeling to comprehend the spatial-temporal variability in hearing loss induced by the mumps virus. Our goal is to depict the complex dynamics of auditory impairment by using fractional calculus, considering the long-range interactions and memory that are intrinsic to viral infections. By focusing on the spatial and temporal features of the development of hearing loss, our work goes beyond traditional epidemiological models and provides insight into the complex evolution of hearing loss over time and geography. One of the main goals of our work is to improve the theoretical foundations of epidemiological modeling and fractal calculus by comprehensively investigating the existence and uniqueness of solutions within Caputo's fractal model. Furthermore, we use the Laplace residual power series (LRPS) method to derive numerical solutions, providing a computationally efficient way to investigate the dynamics of mumps-associated hearing loss. Our study advances both fields by combining mathematical models with epidemiological observations. It provides important insights into the mechanisms underlying mumps-induced hearing loss, and directs future approaches to diagnosis, treatment, and prevention.

The paper organizes as introduction in the first section. Section 2 devoted to presenting the definition of Caputo fractional derivative and their essential properties. Moreover, we present the basic idea of the LRPS method in the same section. The existence and uniqueness of the proposed fractional model of mumps-induced hearing loss investigated in Section 3. The proposed methodology, LRPS method, utilizing to construct numerical solutions for the governing model in Section 4. Section 5 presents a discussion about the obtained results. Finally, some conclusions and future recommendations are provided in Section 6.

2 Preliminaries

2.1 Fractional Calculus

Integer-order differential equations are frequently used in conventional ecological models to characterize the dynamics of species populations. These models, however, have the potential to oversimplify the dynamics, particularly when addressing systems that display memory, genetic effects, or distant interactions. By introducing fractional-order derivatives and integrals, fractional calculus offers a more sophisticated framework that makes it possible to reflect ecological processes in the actual world more accurately. Fractional derivatives have various definitions, each with advantages and uses of their own. In our work, we consider the Caputo fractional derivative.

Definition 1. [16] For an integrable function ψ, the Caputo derivative of fractional order $\beta \in (0,1)$ is given by:

$$D_t^{\beta}\psi(t) = \frac{1}{\Gamma(m-\beta)}\int_0^t \frac{\partial^m \psi(t)}{\partial t^m}\frac{1}{(t-\tau)^{\beta-m+1}}\,d\tau, \quad (9)$$

where $t \geq 0$, $m = \lfloor\beta\rfloor + 1$. The Riemann-Liouville fractional integral of order β, $\mathrm{Re}(\beta) > 0$, is given by:

$$I_t^{\beta}\psi(t) = \frac{1}{\Gamma(\beta)}\int_0^t (t-\tau)^{\beta-1}\psi(\tau)\,d\tau. \quad (10)$$

Lemma 1. [16] For $0 < \beta < 1$ and $t \geq 0$, we get the following property for the Caputo derivative:

$$I_t^{\beta}D_t^{\beta}\psi(t) = \psi(t) - \sum_{i=0}^{m-1}\frac{d^i\psi(0)}{dt^i}\frac{t^i}{i!}. \quad (11)$$

Definition 2. [16] Let $\psi(t)$ be a piecewise continuous function on $[0,\infty)$ and of exponential order η. The Laplace transformation (LT) of $\psi(t)$ is defined as:

$$\Psi(s) = L\{\psi(t)\} = \int_0^{\infty} e^{-st}\psi(t)\,dt, \quad s > \eta, \quad (12)$$

while the inverse Laplace transformation of $\Psi(s,x)$ is given by:

$$\psi(t) = L^{-1}\{\Psi(s)\} = \int_{v-i\infty}^{v+i\infty} e^{st}\Psi(s)\,ds, \quad v = \mathrm{Re}(s) > v_0, \quad (13)$$

where v_0 lies in the right half-plane of the absolute convergence of the Laplace integral.

Lemma 2. [17] Let $\psi(t)$ be a piecewise continuous function on $[0,\infty)$ and of exponential order η, and $\Psi(s) = L\{\psi(t)\}$. Then:

1. $\lim_{s\to\infty} s\Psi(s) = \psi(0)$.
2. $L\{I_t^{\beta}\psi(t)\} = \frac{\Psi(s)}{s^{\beta}}, \quad \beta > 0$.
3. $L\{D_t^{\beta}\psi(t)\} = s^{\beta}\Psi(s) - \sum_{i=0}^{m-1} s^{\beta-i-1}\frac{d^i\psi(0)}{dt^i}$.

2.2 Laplace Residual Power Series Method

Fractional differential equations require special methods so that we can derive and extract exact or numerical solutions due to the complexities we face when considering fractional derivatives in the systems being studied. This urgent need prompted scientists and researchers to provide and develop effective and appropriate methods to reach the desired solutions. For instance, the finite difference approaches [18], multistep approach [19], iterative reproducing kernel method [20], the generalized Taylor's formula [21], multistep generalized differential transform method [**?**], Fractional residual series method [23], homotopy analysis method [24], Jacobi Polynomials approach [25], and Legendre polynomials approach [26]. The LRPS technique is a mathematical strategy for solving fractional differential equations [27]. It offers a disciplined approach to solving equations with fractional derivatives analytically. The method involves solving the original equation in the time domain by applying inverse Laplace transforms after translating it into the Laplace domain, expressing it as a power series, and analyzing the residual series. It is a crucial tool in fields such as applied mathematics, engineering, and physics because it is particularly useful when traditional analytical methods fail to solve difficult fractional calculus problems [28]-[31].

Theorem 1. [32] Let $\psi(t)$ be a piecewise continuous function on $[0,\infty)$ and of exponential order η, and $\Psi(s)=L\{\psi(t)\}$. Then the transformed function $\Psi(s)$ can be represented in the following expansion:

$$\Psi(s)=\sum_{j=0}^{\infty}\frac{b_j}{s^{1+j\beta}},\quad 0<\beta\leq 1,\quad s>\eta, \tag{14}$$

where the coefficients $b_j=D_t^{j\beta}\psi(0)$, $j=0,1,2,\ldots$. Moreover, the inverse Laplace transformation of the expansion (14) can be given as:

$$\psi(t)=\sum_{j=0}^{\infty}\frac{D_t^{j\beta}\psi(0)}{\Gamma(j\beta+1)}t^{i\alpha}. \tag{15}$$

Furthermore, if $|sL\{D_t^{(j+1)\beta}\psi(t)\}|<M$ on $0<s\leq d$, where $0<\beta\leq 1$, then the remainder $R_j(s)$ of the expression (15) satisfies the following:

$$|R_j(s)|\leq\frac{M}{s^{(j+1)\beta+1}},\quad 0<s\leq d. \tag{16}$$

Now, we present the algorithm for the LRPS method of nonlinear fractional differential equations (NFDEs).

Algorithm. LRPS Method for the NFDEs

1. Consider the following NFDEs:

$$D_t^{\beta}\psi_i(t)-N_i(\psi_1,\psi_2,\ldots,\psi_K)-f_i(t)=0,\quad i=1,2,\ldots,K, \tag{17}$$

subject to the initial conditions:

$$\psi_i(0)=g_{i0},\quad i=1,2,\ldots,K, \tag{18}$$

where D_t^{β} is the Caputo derivative of order β ($0<\beta<1$) with respect to t, and N_i, $i=1,2,\ldots,K$, are well-known nonlinear analytical functions.

2. Applying LT to both sides of (17) with the aid of Lemma 2 to get:

$$\Psi_i(s)-\frac{1}{s}g_{i0}-\frac{1}{s^{\beta}}N_Li(s)-\frac{1}{s^{\beta}}F_i(s)=0,\quad i=1,2,\ldots,K, \tag{19}$$

where $\Psi_i(s)=L\{\psi_i(t)\}$, $N_Li(s)=L\{N_i(\psi_1,\psi_2,\ldots,\psi_K)\}$, and $F_i(s)=L\{f_i(t)\}$, $i=1,2,\ldots,K$.

3. The solutions of system (19) are assumed to be in the form:

$$\Psi_i(s)=\sum_{j=0}^{\infty}\frac{b_{ij}}{s^{j\beta+1}},\quad s>0,\quad i=1,2,\ldots,K, \tag{20}$$

where b_{ij} are coefficients to be determined. Using part (1) of Lemma 2 to obtain the initial coefficient in the series (20) as $b_{i0}=g_{i0}$, we can write the solutions of system (19) as:

$$\Psi_i(s)=\frac{g_{i0}}{s}+\sum_{j=1}^{\infty}\frac{b_{ij}}{s^{j\beta+1}},\quad s>0,\quad i=1,2,\ldots,K. \tag{21}$$

4. Define the N-th truncated series of $\Psi_i(s)$ as:

$$\Psi_i^N(s)=\frac{g_{i0}}{s}+\sum_{j=1}^{N-1}\frac{b_{ij}}{s^{j\beta+1}},\quad s>0,\quad i=1,2,\ldots,K. \tag{22}$$

5. Define the Laplace residual functions:

$$LRes_i(s)=\Psi_i(s)-\frac{1}{s}g_{i0}-\frac{1}{s^{\beta}}N_Li(s)-\frac{1}{s^{\beta}}F_i(s), \tag{23}$$

for $i=1,2,\ldots,K$, where $\Psi_i(s)$ as in (21). Additionally, define the N-th Laplace residual functions as:

$$LRes_i^N(s)=\Psi_i^N(s)-\frac{1}{s}g_{i0}-\frac{1}{s^{\beta}}N_Li(s)-\frac{1}{s^{\beta}}F_i(s), \tag{24}$$

for $i=1,2,\ldots,K$, where $\Psi_i^N(s)$ as in (22).

6. Multiply (24) by $s^{j\beta+1}$, $j=1,2,\ldots$, and solve the obtained algebraic system:

$$\lim_{s\to\infty}s^{j\beta+1}LRes_i^j(s)=0,\quad j=1,2,\ldots,\quad i=1,2,\ldots,K. \tag{25}$$

to determine the coefficients $b_{i1},b_{i2},\ldots,b_{i(N-1)}$, $i=1,2,\ldots,K$.

7. Substitute the inferred coefficients $b_{ij}, j=1,2,\ldots,N, i=1,2,\ldots,K$ in (22) to obtain the N-th solutions for $\Psi_i(s)$, $i=1,2,\ldots,K$.

8. Apply the inverse LT to the obtained $\Psi_i(s)$, $i=1,2,\ldots,K$, in Step 7, using Theorem 1 to obtain the N-th LRPS solutions $\psi_i(t)$ for the NFDEs (17) in the form:

$$\psi_i(t)=g_{i0}+\sum_{j=1}^{N-1}\frac{b_{ij}}{\Gamma(j\beta+1)}t^{i\alpha}. \tag{26}$$

3 Existence and uniqueness of solution

The fixed-point theorem is one of the basic ideas in mathematics, which states that there is a point that does not change when it undergoes a certain transformation [33]. The presence of derivatives with non-integer order in fractional differential equations is a real challenge in proving the existence of solutions to this type of equation [34]. The fixed-point theorem can be used to help us reach this goal by reformulating the fractional differential equation as a fixed-point problem [35]. Therefore, the fixed-point theory is considered an essential tool to make our knowledge more extensive in the field of fractional calculus and its many applications in many scientific and engineering fields [36,37]. In this section, we use fixed-point theory to investigate the existence of solutions to the fractional model of mumps-induced hearing loss (5)-(8). Define the following kernels:

$$K_S(t,\psi_S)=\mu-\alpha_1\psi_S(t)\psi_L(t)-\alpha_2\psi_S(t)+\alpha_3\psi_R(t), \tag{27}$$

$$K_L(t,\psi_L) = \alpha_1\psi_S(t)\psi_L(t) - \alpha_2\psi_L(t) - \alpha_4\psi_L(t), \quad (28)$$

$$K_R(t,\psi_R) = \alpha_4\psi_L(t) - \alpha_3\psi_R(t) - \alpha_2\psi_R(t). \quad (29)$$

Consequently, the fractional model of mumps-induced hearing loss (5)-(7) can be written as:

$$\frac{1}{\delta^{1-\beta}} D_t^\beta \psi_S = K_S(t,\psi_S), \quad (30)$$

$$\frac{1}{\delta^{1-\beta}} D_t^\beta \psi_L = K_L(t,\psi_L), \quad (31)$$

$$\frac{1}{\delta^{1-\beta}} D_t^\beta \psi_R = K_R(t,\psi_R). \quad (32)$$

With the help of Lemma 1 and the initial conditions (8), we can apply the Riemann-Liouville fractional integral to both sides of (30)-(32) and obtain:

$$\psi_S(t) - \psi_{S0} = \frac{\delta^{1-\beta}}{\Gamma(\beta)} \int_0^t K_S(t,\psi_S)(t-\tau)^{\beta-1} d\tau, \quad (33)$$

$$\psi_L(t) - \psi_{L0} = \frac{\delta^{1-\beta}}{\Gamma(\beta)} \int_0^t K_L(t,\psi_L)(t-\tau)^{\beta-1} d\tau, \quad (34)$$

$$\psi_R(t) - \psi_{R0} = \frac{\delta^{1-\beta}}{\Gamma(\beta)} \int_0^t K_R(t,\psi_R)(t-\tau)^{\beta-1} d\tau. \quad (35)$$

We look forward to proving that the kernels $K_S(t,\psi_S)$, $K_L(t,\psi_L)$, and $K_R(t,\psi_R)$ in (27)-(29) satisfy the Lipschitz condition. For this purpose, we consider the following assumption:

Assumption A: For the continuous functions $\psi_S(t)$, $\psi_L(t)$, and $\psi_R(t)$ belonging to $L[0,1]$, there exist constants $\gamma_i \in \mathbb{N}, i = 1,2,3$, such that the following hold true:

$$\|\psi_S(t)\| < \gamma_1, \quad \|\psi_L(t)\| < \gamma_2, \quad \|\psi_R(t)\| < \gamma_3. \quad (36)$$

Now we are ready to present the following result.

Theorem 2: The kernels $K_S(t,\psi_S)$, $K_L(t,\psi_L)$, and $K_R(t,\psi_R)$ in (27)-(29) satisfy the Lipschitz condition and contraction, provided that assumption A and the following inequalities are satisfied:

$$\Delta_1 = \alpha_1\gamma_2 + \alpha_2 < 1, \quad (37)$$

$$\Delta_2 = \alpha_1\gamma_1 + \alpha_2 + \alpha_4 < 1, \quad (38)$$

$$\Delta_3 = \alpha_2 + \alpha_3 < 1. \quad (39)$$

Proof: For $\psi_S(t)$ and $\psi_S^*(t)$, using the definition of $K_S(t,\psi_S)$ in (27) with the aid of assumption A, we get:

$$\begin{aligned}
&\|K_S(t,\psi_S) - K_S(t,\psi_S^*)\| = \\
&\|\mu - \alpha_1\psi_S(t)\psi_L(t) - \alpha_2\psi_S(t) + \alpha_3\psi_R(t) - \\
&(\mu - \alpha_1\psi_S^*(t)\psi_L(t) - \alpha_2\psi_S^*(t) + \alpha_3\psi_R(t))\| = \\
&\| - \alpha_1\psi_L(t)(\psi_S(t) - \psi_S^*(t)) - \alpha_2(\psi_S(t) - \psi_S^*(t))\| \\
&\le (\alpha_1\|\psi_L(t)\| + \alpha_2)\|\psi_S(t) - \psi_S^*(t)\| < \\
&(\alpha_1\gamma_2 + \alpha_2)\|\psi_S(t) - \psi_S^*(t)\| = \Delta_1\|\psi_S(t) - \psi_S^*(t)\|. \quad (40)
\end{aligned}$$

Regarding the kernel $K_L(t,\psi_L)$ in (28), we obtain the following for $\psi_L(t)$ and $\psi_L^*(t)$:

$$\begin{aligned}
&\|K_L(t,\psi_L) - K_L(t,\psi_L^*)\| = \\
&\|\alpha_1\psi_S(t)\psi_L(t) - \alpha_2\psi_L(t) - \alpha_4\psi_L(t) - \\
&(\alpha_1\psi_S(t)\psi_L^*(t) - \alpha_2\psi_L^*(t) - \alpha_4\psi_L^*(t))\| = \\
&\|\alpha_1\psi_S(t)(\psi_L(t) - \psi_L^*(t)) - (\alpha_2 + \alpha_4)(\psi_L(t) - \psi_L^*(t))\| \\
&\le (\alpha_1\|\psi_S(t)\| + \alpha_2 + \alpha_4)\|\psi_L(t) - \psi_L^*(t)\| < \\
&(\alpha_1\gamma_1 + \alpha_2 + \alpha_4)\|\psi_L(t) - \psi_L^*(t)\| = \Delta_2\|\psi_L(t) - \psi_L^*(t)\|
\end{aligned} \quad (41)$$

For the continuous functions $\psi_R(t)$ and $\psi_R^*(t)$, we obtain the following result for the kernel $K_R(t,\psi_R)$ in (29):

$$\begin{aligned}
&\|K_R(t,\psi_R) - K_R(t,\psi_R^*)\| = \\
&\|\alpha_4\psi_L(t) - \alpha_3\psi_R(t) - \alpha_2\psi_L(t) - \\
&(\alpha_4\psi_L(t) - \alpha_3\psi_R^*(t) - \alpha_2\psi_R^*(t))\| = \\
&\| - (\alpha_2 + \alpha_3)(\psi_R(t) - \psi_R^*(t))\| = \\
&(\alpha_2 + \alpha_3)\|\psi_R(t) - \psi_R^*(t)\| = \Delta_3\|\psi_R(t) - \psi_R^*(t)\| \quad (42)
\end{aligned}$$

Using the obtained results in (40)-(42) and the inequalities (37)-(39), we conclude that the kernels $K_S(t,\psi_S)$, $K_L(t,\psi_L)$, and $K_R(t,\psi_R)$ satisfy the Lipschitz condition and contraction. The proof is complete.

For $\psi_M(t)$, $\psi_L(t)$, $\psi_A(t)$, and $\psi_Z(t)$, we define the difference between two subsequent components as follows:

$$\hat{\psi}_S^k(t) = \psi_S^k(t) - \psi_S^{k-1}(t) = \frac{1}{\Gamma(\beta)} \int_0^t \left(K_S(t,\psi_S^{k-1}) - K_S(t,\psi_S^{k-2})\right)(t-\tau)^{\beta-1} d\tau \quad (43)$$

$$\hat{\psi}_L^k(t) = \psi_L^k(t) - \psi_L^{k-1}(t) = \frac{1}{\Gamma(\beta)} \int_0^t \left(K_L(t,\psi_L^{k-1}) - K_L(t,\psi_L^{k-2})\right)(t-\tau)^{\beta-1} d\tau \quad (44)$$

$$\hat{\psi}_R^k(t) = \psi_R^k(t) - \psi_R^{k-1}(t) = \frac{1}{\Gamma(\beta)} \int_0^t \left(K_R(t,\psi_R^{k-1}) - K_R(t,\psi_R^{k-2})\right)(t-\tau)^{\beta-1} d\tau \quad (45)$$

Upon these definitions, we conclude that:

$$\psi_S^k(t) = \sum_{j=0}^{k} \hat{\psi}_S^k(t), \quad (46)$$

$$\psi_L^k(t)=\sum_{j=0}^{k}\hat{\psi}_L^k(t), \tag{47}$$

$$\psi_R^k(t)=\sum_{j=0}^{k}\hat{\psi}_R^k(t), \tag{48}$$

Now, we can present the following theorem.

Theorem 3. The fractional model of mumps-induced hearing loss (5)-(8) has a solution provided that the assumption A, the inequalities in (37)-(39), and the following inequality hold true:

$$\Delta^*=\max_{i=1,2,3}\Delta_i<1. \tag{49}$$

Proof. Since the kernel $K_S(t,\psi_S)$ in (27) satisfies the Lipschitz condition, and using (43), we get:

$$\begin{aligned}\left\|\hat{\psi}_S^k(t)\right\| &= \left\|\psi_S^k(t)-\psi_S^{k-1}(t)\right\| = \\ &\left\|\frac{1}{\Gamma(\beta)}\int_0^t\left(K_S(t,\psi_S^{k-1})-K_S(t,\psi_S^{k-2})\right)(t-\tau)^{\beta-1}d\tau\right\| \leq \\ &\frac{1}{\Gamma(\beta)}\int_0^t\left\|\left(K_S(t,\psi_S^{k-1})-K_S(t,\psi_S^{k-2})\right)(t-\tau)^{\beta-1}\right\|d\tau < \\ &\frac{1}{\Gamma(\beta)}\Delta_1\int_0^t\left\|\hat{\psi}_S^{k-1}(\tau)\right\|d\tau\end{aligned} \tag{50}$$

Similarly, we obtain the following:

$$\|\hat{\psi}_L^k(t)\|<\frac{1}{\Gamma(\beta)}\Delta_2\int_0^t\|\hat{\psi}_L^{k-1}(\tau)\|d\tau, \tag{51}$$

$$\|\hat{\psi}_R^k(t)\|<\frac{1}{\Gamma(\beta)}\Delta_3\int_0^t\|\hat{\psi}_R^{k-1}(\tau)\|d\tau. \tag{52}$$

Define the following differences:

$$T_S^k(t)=\psi_S^{k+1}(t)-\psi_S(t), \tag{53}$$

$$T_L^k(t)=\psi_L^{k+1}(t)-\psi_L(t), \tag{54}$$

$$T_R^k(t)=\psi_R^{k+1}(t)-\psi_R(t). \tag{55}$$

Using (49) and (50), we obtain:

$$\begin{aligned}\left\|T_S^k(t)\right\| &= \left\|\psi_S^{k+1}(t)-\psi_S(t)\right\| < \\ &\left(\frac{1}{\Gamma(\beta)}\Delta_1\right)^k\left\|\psi_S^1(t)-\psi_S(t)\right\| < \\ &\left(\frac{1}{\Gamma(\beta)}\Omega^*\right)^k\left\|\psi_S^1(t)-\psi_S(t)\right\|\end{aligned} \tag{56}$$

In a similar way, we infer the following:

$$\|T_L^k(t)\|<\left(\frac{1}{\Gamma(\beta)}\Omega^*\right)^k\|\psi_L^1(t)-\psi_L(t)\|, \tag{57}$$

$$\|T_R^k(t)\|<\left(\frac{1}{\Gamma(\beta)}\Omega^*\right)^k\|\psi_R^1(t)-\psi_R(t)\|. \tag{58}$$

It is obvious that when $k\to\infty$, we get $T_S^k(t)\to 0$, $T_L^k(t)\to 0$, and $T_R^k(t)\to 0$. This completes the proof. □

We seek to prove the uniqueness of the solution of the fractional model of mumps-induced hearing loss (5)-(8) through the following theorem.

Theorem 4. The fractional model of mumps-induced hearing loss (5)-(8) has a unique solution if the assumption A, the inequalities in (37)-(39), and the following conditions hold true:

$$\frac{1}{\Gamma(\beta)}\Delta_i\leq 0,\quad \text{for } i=1,2,3. \tag{59}$$

Proof. Assume that the fractional model of mumps-induced hearing loss (5)-(8) has another pair of solutions $\psi_S^*(t),\psi_L^*(t),\psi_R^*(t)$. According to (33), $\psi_S^*(t)$ satisfies the following integral equation:

$$\psi_S^*(t)=\psi_S0+\frac{1}{\Gamma(\beta)}\int_0^t K_S(t,\psi_M^*)(t-\tau)^{\beta-1}d\tau, \tag{60}$$

Consequently, using the result in (50) to obtain:

$$\begin{aligned}&\|\psi_S(t)-\psi_S^*(t)\|\leq \\ &\frac{1}{\Gamma(\beta)}\int_0^t\left\|(K_S(t,\psi_M)-K_S(t,\psi_M^*))(t-\tau)^{\beta-1}\right\|d\tau \\ &\leq\frac{1}{\Gamma(\beta)}\Delta_1\|\psi_S(t)-\psi_S^*(t)\|\end{aligned} \tag{61}$$

This gives:

$$\left(1-\frac{1}{\Gamma(\beta)}\Delta_1\right)\|\psi_S(t)-\psi_S^*(t)\|\leq 0. \tag{62}$$

Using this result and the condition in (59), we obtain $\psi_S(t)=\psi_S^*(t)$. We can obtain the uniqueness of $\psi_S(t)$. Similarly, we obtain the other results.

4 LRPS scheme for the fractional model of mumps-induced hearing loss

This section is devoted to utilizing the LRPS scheme to establish numerical solutions for the fractional model of mumps-induced hearing loss (5)-(8). Apply the Laplace transformation to both sides of the model (5)-(7) to get:

$$\begin{aligned}&\frac{1}{\delta^{1-\beta}}\mathscr{L}\{D_t^\beta\psi_S\}= \\ &\frac{\mu}{s}-\alpha_1\mathscr{L}\{\psi_S(t)\psi_L(t)\}-\alpha_2\mathscr{L}\{\psi_S(t)\}+\alpha_3\mathscr{L}\{\psi_R(t)\}\end{aligned} \tag{63}$$

$$\begin{aligned}&\frac{1}{\delta^{1-\beta}}\mathscr{L}\{D_t^\beta\psi_L\}= \\ &\alpha_1\mathscr{L}\{\psi_S(t)\psi_L(t)\}-\alpha_2\mathscr{L}\{\psi_L(t)\}-\alpha_4\mathscr{L}\{\psi_L(t)\}\end{aligned} \tag{64}$$

$$\frac{1}{\delta^{1-\beta}}\mathscr{L}\{D_t^{\beta}\psi_R\} = \alpha_4\mathscr{L}\{\psi_L(t)\} - \alpha_3\mathscr{L}\{\psi_R(t)\} - \alpha_2\mathscr{L}\{\psi_R(t)\} \quad (65)$$

We assume $L\{\psi_S(t)\} = \Psi_S(s)$, $L\{\psi_L(t)\} = \Psi_L(s)$, and $L\{\psi_R(t)\} = \Psi_R(s)$. By using Lemma 2 with the aid of the initial conditions in (8), we can rewrite equations (63)-(65) as:

$$\Psi_S(s) = \frac{\psi_{S0}}{s} + \frac{\delta^{1-\beta}}{s^{\beta}}\frac{\mu}{s} - \frac{\delta^{1-\beta}}{s^{\beta}}\alpha_1\mathscr{L}\left\{\mathscr{L}^{-1}\{\Psi_S(s)\}\mathscr{L}^{-1}\{\Psi_L(s)\}\right\} - \frac{\delta^{1-\beta}}{s^{\beta}}\alpha_2\Psi_S(s) + \frac{\delta^{1-\beta}}{s^{\beta}}\alpha_3\Psi_R(s) \quad (66)$$

$$\Psi_L(s) = \frac{\psi_{L0}}{s} + \frac{\delta^{1-\beta}}{s^{\beta}}\left(\alpha_1\mathscr{L}\left\{\mathscr{L}^{-1}\{\Psi_S(s)\}\mathscr{L}^{-1}\{\Psi_L(s)\}\right\} - (\alpha_2+\alpha_4)\Psi_L(s)\right) \quad (67)$$

$$\Psi_R(s) = \frac{\psi_{R0}}{s} + \frac{\delta^{1-\beta}}{s^{\beta}}\left(\alpha_4\Psi_L(s) - \alpha_3\Psi_R(s) - \alpha_2\Psi_R(s)\right) \quad (68)$$

Following Step 3 in the proposed algorithm, the solutions of system (66)-(68) are assumed in the form:

$$\Psi_S(s) = \sum_{i=0}^{\infty}\frac{p_{S,i}}{s^{i\beta+1}}, \quad (69)$$

$$\Psi_L(s) = \sum_{i=0}^{\infty}\frac{p_{L,i}}{s^{i\beta+1}}, \quad (70)$$

$$\Psi_R(s) = \sum_{i=0}^{\infty}\frac{p_{R,i}}{s^{i\beta+1}}. \quad (71)$$

The Nth-truncated solutions are given as:

$$\Psi_S^N(s) = \sum_{i=0}^{N}\frac{p_{S,i}}{s^{i\beta+1}}, \quad (72)$$

$$\Psi_L^N(s) = \sum_{i=0}^{N}\frac{p_{L,i}}{s^{i\beta+1}}, \quad (73)$$

$$\Psi_R^N(s) = \sum_{i=0}^{N}\frac{p_{R,i}}{s^{i\beta+1}}. \quad (74)$$

Using Lemma 2 with initial conditions (8), the initial guess is given by $p_{S,0} = \psi_S 0$, $p_{L,0} = \psi_L 0$, and $p_{R,0} = \psi_R 0$. Consequently, the kth-truncated solutions can be written as:

$$\Psi_S^N(s) = \frac{\psi_S 0}{s} + \sum_{i=1}^{N}\frac{p_{S,i}}{s^{i\beta+1}}, \quad (75)$$

$$\Psi_L^N(s) = \frac{\psi_L 0}{s} + \sum_{i=1}^{N}\frac{p_{L,i}}{s^{i\beta+1}}, \quad (76)$$

$$\Psi_R^N(s) = \frac{\psi_R 0}{s} + \sum_{i=1}^{N}\frac{p_{R,i}}{s^{i\beta+1}}. \quad (77)$$

The LRPS solution for the fractional model of mumps-induced hearing loss (5)-(8) is given by:

$$\psi_S(t) = \psi_{M0} + \frac{p_{(S,1)}}{\Gamma(1+\beta)}t^{\beta} + \frac{p_{(S,2)}}{\Gamma(1+2\beta)}t^{2\beta} + \frac{p_{(S,3)}}{\Gamma(1+3\beta)}t^{3\beta} + \cdots \quad (78)$$

$$\psi_L(t) = \psi_{M0} + \frac{p_{(L,1)}}{\Gamma(1+\beta)}t^{\beta} + \frac{p_{(L,2)}}{\Gamma(1+2\beta)}t^{2\beta} + \frac{p_{(L,3)}}{\Gamma(1+3\beta)}t^{3\beta} + \cdots \quad (79)$$

$$\psi_R(t) = \psi_{M0} + \frac{p_{(R,1)}}{\Gamma(1+\beta)}t^{\beta} + \frac{p_{(R,2)}}{\Gamma(1+2\beta)}t^{2\beta} + \frac{p_{(R,3)}}{\Gamma(1+3\beta)}t^{3\beta} + \cdots \quad (80)$$

5 Numerical results

Here, we validate our analytical inferences using numerical simulations. The software package *Mathematica 13* will be employed to demonstrate our numerical results. Figures 1-3 present the representation of the variations in time series evaluation of population class $\psi_S^{10}(t)$, $\psi_L^{10}(t)$, and $\psi_R^{10}(t)$, respectively. The notation $\psi_S^{10}(t)$ represents the 10th LRPS solution for the number of susceptible individuals who are prone to hearing loss due to genetic disorders, mumps, or any other viral infection, or due to noise. Similarly, $\psi_L^{10}(t)$ and $\psi_R^{10}(t)$ represent the 10th LRPS solution for the number of infected individuals and the number of infected individuals who have recovered from hearing loss, respectively.

We denote RK4 as the solutions obtained by utilizing the 4th order Runge–Kutta method. We use the values of the parameters listed in Table 1 and consider the initial number of susceptible individuals who are prone to hearing loss due to the reasons listed above $\psi_S(0) = 12$, the initial number of infected individuals $\psi_L(0) = 8$, and the initial number of infected individuals who have

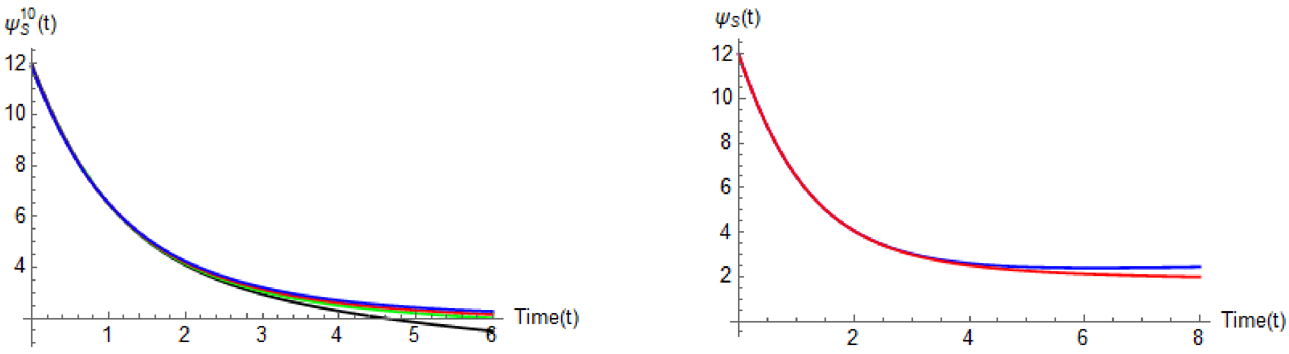

Fig. 1 Represent of the variations in time series evaluation of population class $\psi_S^{10}(t)$ where (a) LRPS solutions at: $\beta = 0.99$; black, $\beta = 0.98$; green, $\beta = 0.97$; red, $\beta = 0.96$; blue, and (b) LRPS solution; red, RK4 solution; blue.

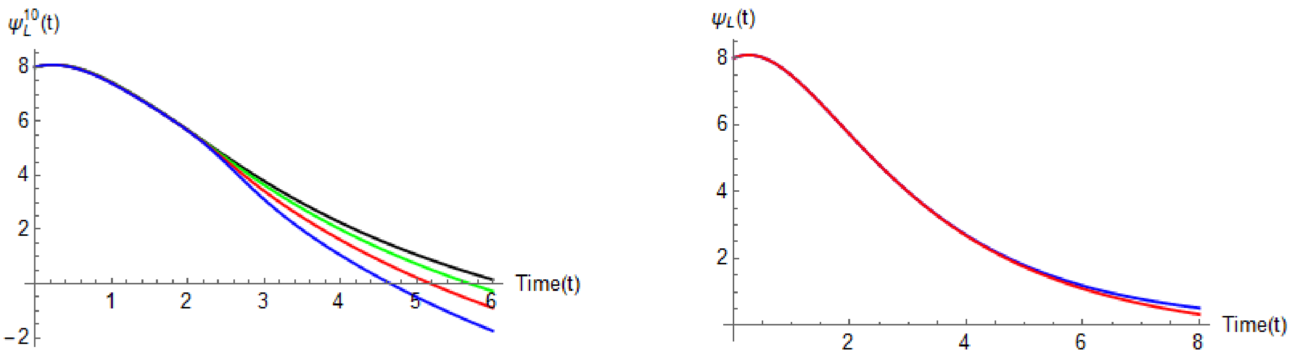

Fig. 2 Representation of the variations in time series evaluation of population class $\psi_L^{10}(t)$ where (a) LRPS solutions at: $\beta = 0.99$; black, $\beta = 0.98$; green, $\beta = 0.97$; red, $\beta = 0.96$; blue, and (b) LRPS solution; red, RK4 solution; blue.

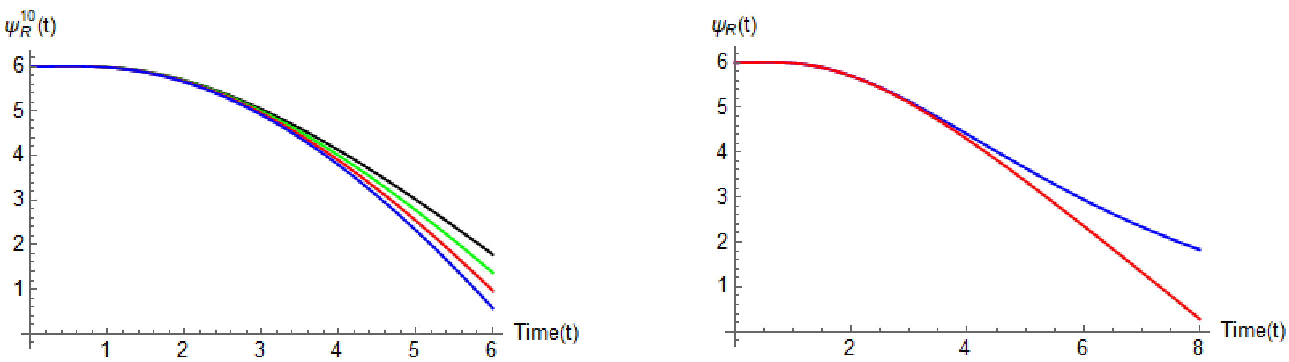

Fig. 3 Representation of the variations in time series evaluation of population class $\psi_R^{10}(t)$ where (a) LRPS solutions at: $\beta = 0.99$; black, $\beta = 0.98$; green, $\beta = 0.97$; red, $\beta = 0.96$; blue, and (b) LRPS solution; red, RK4 solution; blue.

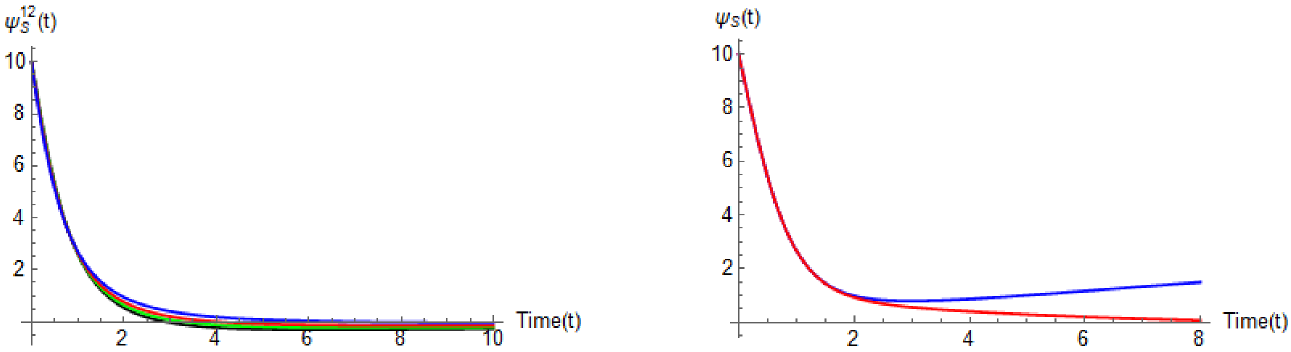

Fig. 4 Represent of the variations in time series evaluation of population class $\psi_S^1 2(t)$ where (a) LRPS solutions at: $\beta = 0.97$; black, $\beta = 0.95$; green, $\beta = 0.93$; red, $\beta = 0.9$; blue and (b) LRPS solution; red, RK4 solution; blue.

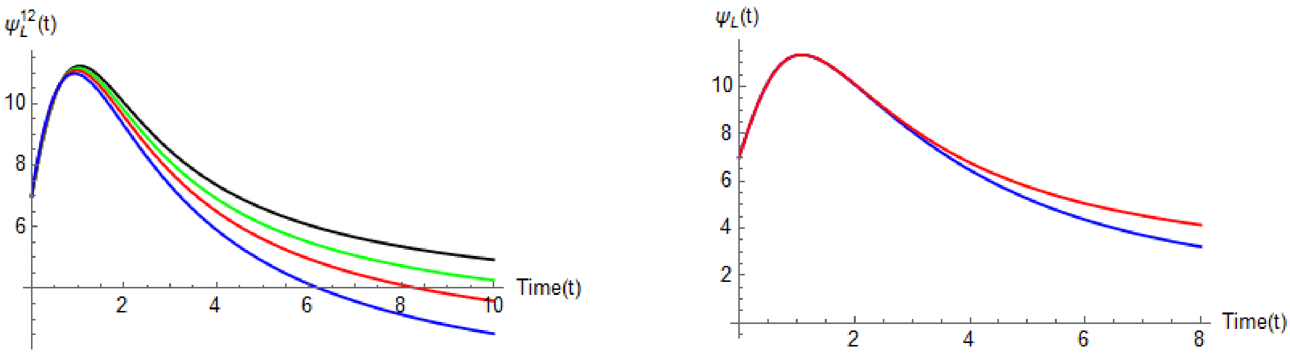

Fig. 5 Represent of the variations in time series evaluation of population class $\psi_L^1 2(t)$ where (a) LRPS solutions at: $\beta = 0.97$; black, $\beta = 0.95$; green, $\beta = 0.93$; red, $\beta = 0.9$; blue and (b) LRPS solution; red, RK4 solution; blue.

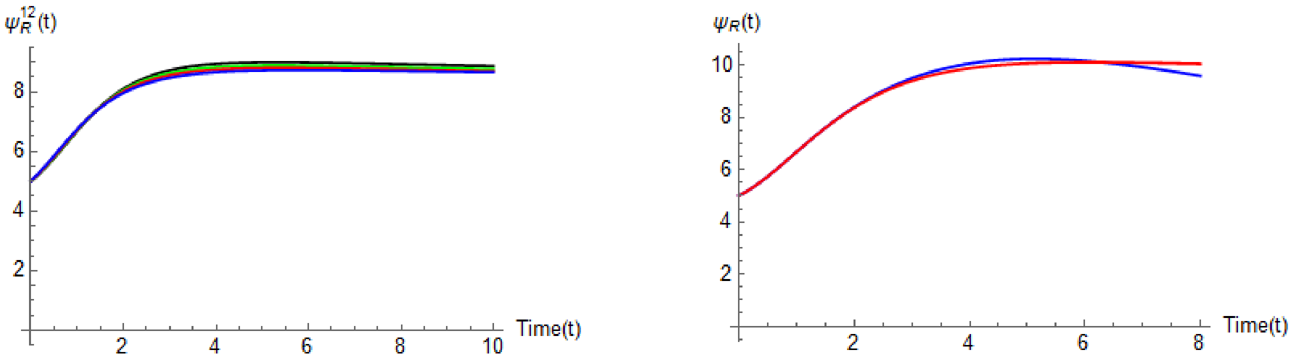

Fig. 6 Represent of the variations in time series evaluation of population class $\psi_R^1 2(t)$ where (a) LRPS solutions at: $\beta = 0.97$; black, $\beta = 0.95$; green, $\beta = 0.93$; red, $\beta = 0.9$; blue and (b) LRPS solution; red, RK4 solution; blue.

Table 2 Numerical results for the population of susceptible individuals of hearing loss, $\psi_S(t)$, at $\beta = 1$.

t	LRPS	RK4	Abs. error	Rel. error
0.0	12.0000000000	12.0000000000	0.000000	0.000000
0.1	11.2468561437	11.2468564149	2.711530×10^{-7}	2.410925×10^{-8}
0.2	10.5439660011	10.5439663465	3.453887×10^{-7}	3.275700×10^{-8}
0.3	9.8897022565	9.8897027886	5.320992×10^{-7}	5.380336×10^{-8}
0.4	9.2821307678	9.2821316553	8.874997×10^{-7}	9.561379×10^{-8}
0.5	8.7190889917	8.7190917076	2.715920×10^{-6}	3.114910×10^{-7}
0.6	8.1982576638	8.1982656892	8.025410×10^{-6}	9.789166×10^{-7}
0.7	7.7172241052	7.7172445213	2.041612×10^{-5}	2.645527×10^{-6}
0.8	7.2735364095	7.2735822114	4.580184×10^{-5}	6.297053×10^{-6}
0.9	6.8647484393	6.8648404804	9.204115×10^{-5}	1.340779×10^{-5}
1.0	6.4884560454	6.4886256471	1.696017×10^{-4}	2.613899×10^{-5}

Table 3 Numerical results for the population of infected individuals, $\psi_L(t)$, at $\beta = 1$.

t	LRPS solution	RK4 solution	Absolute error	Relative error
0.0	8.0000000000	8.0000000000	0.000000	0.000000
0.1	8.0619510293	8.0619508469	1.824238×10^{-7}	2.262775×10^{-8}
0.2	8.0929817110	8.0929814617	2.492485×10^{-7}	3.079810×10^{-8}
0.3	8.0948627960	8.0948624535	3.424605×10^{-7}	4.230590×10^{-8}
0.4	8.0696206885	8.0696205095	1.790050×10^{-7}	2.218258×10^{-8}
0.5	8.0194552196	8.0194551071	1.124384×10^{-7}	1.402070×10^{-8}
0.6	7.9466660119	7.9466659814	3.045808×10^{-8}	3.832813×10^{-9}
0.7	7.8535888647	7.8535890938	2.291076×10^{-7}	2.917235×10^{-8}
0.8	7.7425426887	7.7425431720	4.833607×10^{-7}	6.242919×10^{-8}
0.9	7.6157868267	7.6157880166	1.189895×10^{-6}	1.562408×10^{-7}
1.0	7.4754881071	7.4754908601	2.753045×10^{-6}	3.682763×10^{-7}

Table 4 Numerical results for the population of individuals recovering from hearing loss, $\psi_R(t)$, at $\beta = 1$.

t	LRPS solution	RK4 solution	Absolute error	Relative error
0.0	6.0000000000	6.0000000000	0.000000	0.000000
0.1	6.0015886097	6.0015886172	7.523857×10^{-9}	1.253644×10^{-9}
0.2	6.0042247324	6.0042247338	1.426640×10^{-9}	2.376060×10^{-10}
0.3	6.0071625190	6.0071624999	1.912765×10^{-8}	3.184140×10^{-9}
0.4	6.0097249085	6.0097247746	1.338700×10^{-7}	2.227558×10^{-8}
0.5	6.0113009091	6.0113060494	5.140216×10^{-6}	8.550920×10^{-7}
0.6	6.0113708665	6.0113733408	2.474356×10^{-6}	4.116126×10^{-7}
0.7	6.0094606952	6.0094655263	4.831059×10^{-6}	8.039089×10^{-7}
0.8	6.0051812476	6.0051914415	1.019389×10^{-5}	1.697516×10^{-6}
0.9	5.9982058172	5.9982264355	2.061824×10^{-5}	3.437402×10^{-6}
1.0	5.9882692307	5.9883087047	3.947398×10^{-5}	6.591886×10^{-6}

recovered from hearing loss $\psi_R(0) = 6$. Figures 1(a)-3(a) show the constructed solutions at various fractional derivative orders $\beta = 0.99, 0.98, 0.97$, and 0.96 to illustrate the impact of the fractional derivative on the behavior of the solutions. Whereas Figures 1(b)-3(b) present a comparison between the 10th LRPS solution at $\beta = 1$ and the RK4 solution.

It is clear from Figures 1-3 that the number of susceptible individuals with hearing loss, $\psi_S(t)$, decreases significantly in the time $t \in [0,6]$. While the number of infected individuals, $\psi_L(t)$, increases slightly within a short time, this behavior changes to a decrease in the number of individuals with hearing loss due to the virus during the remaining time. Regarding the number of individuals recovering from hearing loss, $\psi_R(t)$, it remains stable over time $t \in [0,1]$, before decreasing later. These results are consistent with previous studies such as [11,12,13,14].

Tables 2-4 present numerical results for the variations in time series evaluation of population classes $\psi_S(t)$, $\psi_L(t)$, and $\psi_R(t)$, respectively, where the parameters are considered as in Figures 1-3. We present the 10th LRPS solutions and the RK4 solutions at $\beta = 1$. Moreover, we compute the absolute and relative errors between the two methods to validate our results.

From the results presented in these tables, we conclude that the solutions obtained through the proposed approach are very close to those obtained using the RK4 method, indicating the efficiency of the proposed approach in dealing with such important biological systems. The results in Table 2 show that the number of individuals exposed to hearing loss decreased from 12 to 6. Table 3 indicates an increase in the number of individuals suffering from hearing loss due to the virus from time $t = 0$ to $t = 0.3$, followed by a decrease until the number of individuals reached 6 at $t = 1$. Finally, Table 4 shows that the number of people recovering from hearing loss remains relatively stable.

To further investigate our results, we present Figures 4-6, considering different parameter values: $\mu = 0.5$, $\alpha_1 = 0.1433$, $\alpha_2 = 0.1$, $\alpha_3 = 0.02$, and $\alpha_4 = 0.241$. The initial values for the population classes are set as $\psi_S(0) = 10$, $\psi_L(0) = 7$, and $\psi_R(0) = 5$. We depict the 12th LRPS solutions for the population classes, $\psi_S^{12}(t)$, $\psi_L^{12}(t)$, and $\psi_R^{12}(t)$, at various fractional derivative orders $\beta = 0.97, 0.95, 0.93$, and 0.9 in Figures 4(a)-6(a), respectively. A comparison between the obtained solutions using the LRPS method and the RK4 at classical derivative order $\beta = 1$ is presented in Figures 4(b)-6(b). The behavior of these solutions is similar to those presented in Figures 1-3 and aligns with results in previous literature [13].

In conclusion, the results of this study and their comparison with previous research demonstrate the precision and effectiveness of the proposed approach in handling biological models of this magnitude. This motivates us to explore numerical solutions for a variety of complex biological models using the suggested approach. Furthermore, our research provides guidance for future studies on complex models using the Caputo-Fabrizio fractional derivative and conformable derivative as alternative definitions of the fractional derivative.

6 Conclusions

This paper elucidated the performance of fractional Caputo modeling in demonstrating the temporal variations of hearing loss related to the mumps virus. By employing the LRPS approach, we have the potential to construct numerical solutions that expand worthwhile visions into the dynamics of hearing loss. Our presented results confirm the effectiveness of employing fractional calculus to shed light on previously unexplored aspects of the dynamics of hearing loss associated with mumps virus infection. Furthermore, the fact that the solutions we were able to prove in our study are distinct and exist asserts the advantage of fractional calculus in epidemiological modeling. These results upgrade our consciousness of the pathophysiology of mumps-induced hearing loss and aid in improving epidemiological modeling techniques. This work bridges the hole between clinical data and mathematical models, which have significant effects on the handling and treatment of viral infections, particularly those that reduce auditory tasks. The information obtained from this work will be utilized to repair predictive models of infectious disease and promote public health procedures in the future. In addition, our results confirm the significance of the proposed approaches in handling intricate health problems and show how effective it is in integrating mathematical structures like fractional calculus into epidemiological studies.

Acknowledgement

The first author acknowledges the financial support by Zarqa Private University.
The authors are grateful to the anonymous referee for a careful checking of the details and for helpful comments that improved this paper.

References

[1] Shukla, A., Harper, M., Pedersen, E., Goman, A., Suen, J. J., Price, C., ... and Reed, N. S. (2020). Hearing loss, loneliness, and social isolation: a systematic review. Otolaryngology–Head and Neck Surgery, 162(5), 622-633.
[2] Wu, P. Z., O'Malley, J. T., de Gruttola, V., and Liberman, M. C. (2020). Age-related hearing loss is dominated by damage to inner ear sensory cells, not the cellular battery that powers them. Journal of Neuroscience, 40(33), 6357-6366.

[3] Newsted, D., Rosen, E., Cooke, B., Beyea, M. M., Simpson, M. T., and Beyea, J. A. (2020). Approach to hearing loss. Canadian Family Physician, 66(11), 803-809.
[4] Lawrence, B. J., Jayakody, D. M., Bennett, R. J., Eikelboom, R. H., Gasson, N., and Friedland, P. L. (2020). Hearing loss and depression in older adults: a systematic review and meta-analysis. The Gerontologist, 60(3), e137-e154.
[5] Shi, X., Liu, X., and Sun, Y. (2023). The Pathogenesis of Cytomegalovirus and Other Viruses Associated with Hearing Loss: Recent Updates. Viruses, 15(6), 1385.
[6] Karimi-Boroujeni, M., Zahedi-Amiri, A., and Coombs, K. M. (2021). Embryonic origins of virus-induced hearing loss: Overview of molecular etiology. Viruses, 13(1), 71.
[7] Bodewes, R., Reijnen, L., Kerkhof, J., Cremer, J., Schmitz, D., van Binnendijk, R., and Veldhuijzen, I. K. (2020). Molecular epidemiology of mumps viruses in the Netherlands, 2017-2019. Plos one, 15(9), e0233143.
[8] Allen, L. J., Brauer, F., Van den Driessche, P., and Wu, J. (2008). Mathematical epidemiology (Vol. 1945). Berlin: Springer.
[9] Huppert, A., and Katriel, G. (2013). Mathematical modelling and prediction in infectious disease epidemiology. Clinical microbiology and infection, 19(11), 999-1005.
[10] Ojo, M. M., Peter, O. J., Goufo, E. F. D., Panigoro, H. S., and Oguntolu, F. A. (2023). Mathematical model for control of tuberculosis epidemiology. Journal of Applied Mathematics and Computing, 69(1), 69-87.
[11] Davydovych, V., Dutka, V., and Cherniha, R. (2023). Reaction–Diffusion Equations in Mathematical Models Arising in Epidemiology. Symmetry, 15(11), 2025.
[12] Kouilily, F., Aboulkhouatem, F. Z., Yousfi, N., Achtaich, N., and El Khasmi, M. (2018). Modeling the social and epidemiological causes of hearing loss. Revista mexicana de ingeniería biomédica, 39(3), 238-248.
[13] Mohammadi, H., Kumar, S., Rezapour, S., and Etemad, S. (2021). A theoretical study of the Caputo–Fabrizio fractional modeling for hearing loss due to Mumps virus with optimal control. Chaos, Solitons & Fractals, 144, 110668.
[14] Nisar, K. S., Srinivas, M. N., Murthy, B. S. N., Madhusudanan, V., Gul, N., Abdulrehman, J., and Zeb, A. (2023). Exploring the Dynamics of White Noise and Spatial Temporal Variations on Hearing Loss due to Mumps Virus. Results in Physics, 106584.
[15] Hashemi, M. S., Partohaghighi, M., and Ahmad, H. (2023). New mathematical modelings of the human liver and hearing loss systems with fractional derivatives. International Journal of Biomathematics, 16(01), 2250068.
[16] Diethelm, K. (2013). A fractional calculus based model for the simulation of an outbreak of dengue fever. Nonlinear Dynamics, 71, 613-619.
[17] Shafee, A., Alkhezi, Y., & Shah, R. (2023). Efficient Solution of Fractional System Partial Differential Equations Using Laplace Residual Power Series Method. Fractal and Fractional, 7(6), 429.
[18] Edwan, R., Saadeh, R., Hadid, S., Al-Smadi, M., & Momani, S. (2020). Solving time-space-fractional Cauchy problem with constant coefficients by finite-difference method. Computational mathematics and applications, 25-46.
[19] Al-Smadi, M., Freihat, A., Khalil, H., Momani, S., & Ali Khan, R. (2017). Numerical multistep approach for solving fractional partial differential equations. International Journal of Computational Methods, 14(03), 1750029.
[20] El-Ajou, A., Arqub, O. A., & Al-Smadi, M. (2015). A general form of the generalized Taylor's formula with some applications. Applied Mathematics and Computation, 256, 851-859.
[21] Al-Smadi, M. (2018). Simplified iterative reproducing kernel method for handling time-fractional BVPs with error estimation. Ain Shams Engineering Journal, 9(4), 2517-2525.
[22] Momani, S., Freihat, A., & Al-Smadi, M. (2014). Analytical study of fractional-order multiple chaotic Fitzhugh-Nagumo neurons model using multistep generalized differential transform method. In Abstract and Applied Analysis (Vol. 2014, pp. 1-10). Hindawi Limited.
[23] Al-Smadi, M. (2021). Fractional residual series for conformable time-fractional Sawada–Kotera–Ito, Lax, and Kaup–Kupershmidt equations of seventh order. Mathematical Methods in the Applied Sciences.
[24] AL-Smadi, M. H., & Gumah, G. N. (2014). On the homotopy analysis method for fractional SEIR epidemic model. Research Journal of Applied Sciences, Engineering and Technology, 7(18), 3809-3820.
[25] Khalil, H., Khan, R. A., H Al-Smadi, M., & A Freihat, A. (2020). Approximation of solution of time fractional order three-dimensional heat conduction problems with Jacobi Polynomials. Punjab University Journal of Mathematics, 47(1).
[26] Altawallbeh, Z., Al-Smadi, M., & Abu-Gdairi, R. (2013). Approximate solution of second-order integrodifferential equation of Volterra type in RKHS method. International Journal of Mathematical Analysis, 7(44), 2145-2160.
[27] Oqielat, M. A. N., Eriqat, T., Ogilat, O., El-Ajou, A., Alhazmi, S. E., & Al-Omari, S. (2023). Laplace-Residual Power Series Method for Solving Time-Fractional Reaction–Diffusion Model. Fractal and Fractional, 7(4), 309.
[28] Alaroud, M. (2022). Application of Laplace residual power series method for approximate solutions of fractional IVP's. Alexandria Engineering Journal, 61(2), 1585-1595.
[29] Alderremy, A. A., Shah, R., Iqbal, N., Aly, S., & Nonlaopon, K. (2022). Fractional Series Solution Construction for Nonlinear Fractional Reaction-Diffusion Brusselator Model Utilizing Laplace Residual Power Series. Symmetry, 14(9), 1944.
[30] Sarhan, A., Burqan, A., Saadeh, R., & Al-Zhour, Z. (2022). Analytical Solutions of the Nonlinear Time-Fractional Coupled Boussinesq-Burger Equations Using Laplace Residual Power Series Technique. Fractal and Fractional, 6(11), 631.
[31] Alquran, M., Alsukhour, M., Ali, M., & Jaradat, I. (2021). Combination of Laplace transform and residual power series techniques to solve autonomous n-dimensional fractional nonlinear systems. Nonlinear Engineering, 10(1), 282-292.
[32] Shafee, A., Alkhezi, Y., & Shah, R. (2023). Efficient Solution of Fractional System Partial Differential Equations Using Laplace Residual Power Series Method. Fractal and Fractional, 7(6), 429.
[33] Mebarki, K., Georgiev, S., Djebali, S., & Zennir, K. (2023). Fixed Point Theorems with Applications. CRC Press.
[34] Ali, A., Sarwar, M., Zada, M. B., & Shah, K. (2021). Existence of solution to fractional differential equation with fractional integral type boundary conditions. Mathematical Methods in the Applied Sciences, 44(2), 1615-1627.

[35] Abdo, M. S., Abdeljawad, T., Ali, S. M., Shah, K., & Jarad, F. (2020). Existence of positive solutions for weighted fractional order differential equations. Chaos, Solitons & Fractals, 141, 110341.

[36] Dzherbashian, M. M., & Nersesian, A. B. (2020). Fractional derivatives and Cauchy problem for differential equations of fractional order. Fractional Calculus and Applied Analysis, 23(6), 1810-1836.

[37] Verma, P., & Kumar, M. (2022). An analytical solution of linear/nonlinear fractional-order partial differential equations and with new existence and uniqueness conditions. Proceedings of the National Academy of Sciences, India Section A: Physical Sciences, 92(1), 47-55.

Siham Ayasrah Researcher in the field of applied hearing at Zarqa Private University. Her research focuses on methods of treating hearing-related diseases and employing applied sciences in her specific field.

Asad Freihat Associate Professor of Applied Mathematics at Al-Balqa Applied University. He has made significant contributions to the development of numerical methods for dealing with biological systems in the context of fractional derivatives. He is very distinguished in building the code for the mathematical software package Mathematica.

Mohammed Alabedalhadi Assistant Professor of Applied Mathematics at Al-Balqa Applied University. His research interests focus on developing methods and approaches to derive accurate and approximate solutions to ordinary and partial fractional differential equations. He has numerous researches in the field of traveling wave solutions to equations that appear in quantum physics and other important sciences.

Mohammed Al-Smadi He holds a professorship in applied mathematics at Al-Balqa Applied University. He was selected to join the most cited scientists in 2024, as he has a large number of diverse scientific research in various fields of applied mathematics, published in a wide range of peer-reviewed scientific journals.

Shrideh Al-Omari He holds a professorship in applied mathematics at Al-Balqa Applied University. He was selected to join the most cited scientists in 2024, as he has a large number of diverse scientific research in various fields of applied mathematics, published in a wide range of peer-reviewed scientific journals.

Dumitru Baleanu He is a mathematician known for his contributions to fractional calculus and dynamical systems. He currently serves as a professor at several universities and research institutions, and has published numerous scientific papers and books in the field. His work is used in diverse applications such as physics, engineering, and computer science.